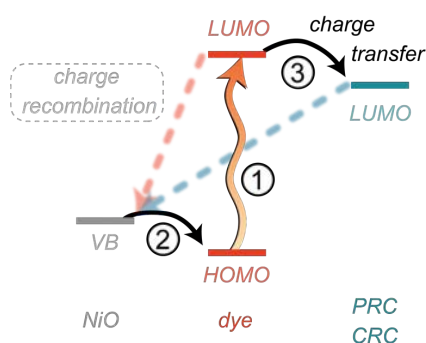


As a result of climate change and pollution, humanity is in search of alternative ways to generate, use and store energy. Preferably, our energy originates only from renewable sources in the future, and the fuels we use for energy storage and transport will be based on non-polluting chemical building blocks. H<sub>2</sub>O and CO<sub>2</sub> are very abundant chemical feedstocks that could serve this purpose, and can be converted to fuels using sunlight as the renewable source. Their conversion into so-called *solar fuels*, also known as artificial photosynthesis, commonly takes place in photoelectrochemical (PEC) cells. The most efficient PEC cells known to date commonly employ precious metals in the photoelectrode. Due to the size of the energy sector, less scarce materials should be used instead, such as first-row transition metals.

Dye-sensitized photoelectrochemical cells (DSPECs) enable the use of non-precious metals in photoelectrodes, as was discussed in **Chapter 1**. Photosensitizers and molecular catalysts based on organic molecules or first-row transition metal complexes can harvest sunlight and catalyze hydrogen production or CO<sub>2</sub> conversion. Unfortunately, the efficiency and stability of DSPECs is still low, and is greatly hampered by the poor performance of the photocathode.

The dye-sensitized photocathode consists of three components (Figure 1): a *p*-type semiconducting material (commonly NiO), a photosensitizer (dye) for light harvesting, and a molecular catalyst to catalyze the half-reaction of interest (e.g., proton reduction to hydrogen). The electron transfers between these three components (depicted as black arrows) ideally proceed in a synchronized fashion, like a clockwork. In reality, the time scales at which these electron transfers occur, differ in orders of magnitude, which leads to a loss in efficiency due to undesired side reactions, such as charge recombination (Figure 1, dashed arrows) and catalyst decomposition. In this dissertation, we address above issues by introducing novel dye-sensitized (photo)cathodes for solar fuel production. Chapters 2 and 3 describe fundamental studies that were essential to realize the (photo)cathodes described in Chapters 4 to 6.



**Figure 1.** Schematic depiction of the working principle of the dye-sensitized photocathode, consisting of a *p*-type semiconductor (NiO), a photosensitizer (dye) and a proton or CO<sub>2</sub> reduction catalyst (PRC or CRC, respectively). Electron transfers are indicated by the solid arrows and the expected order at which they occur is indicated by the numbers. Charge recombination is indicated by the dashed arrows.

At the fundamentals of the dye-sensitized photocathode lies the NiO electrode, and the aim of **Chapter 2** was to understand how this material functions optimally. We have studied the performance of the NiO electrodes prepared in our lab in a benchmark dye-sensitized solar cell, based on the P1 dye and the  $I^-/I_3^-$  redox couple. The thickness of the NiO electrode was varied, and it was found that the benchmark solar cells reached the highest efficiency when four layers of NiO were applied on top of each other. The solar cell efficiency was found to be directly correlated to the short circuit current of the solar cell. To obtain deeper insight into the origin of this optimum at four NiO layers, the charge dynamics of the photocathodes were investigated *in operando*, using photoelectrochemical impedance spectroscopy. It was shown that more NiO layers led to a higher photosensitizer loading, and thus more efficient light harvesting. Simultaneously, the poor hole conductivity of NiO led to a poorer collection of the photogenerated hole in the thicker NiO layers (Figure 2, green path). If the photocathode contains more than four layers of NiO, the beneficial increase in light harvesting is counteracted by the decreasing ability of the electrode to collect the photogenerated holes, leading to the optimal performance at four layers of NiO.

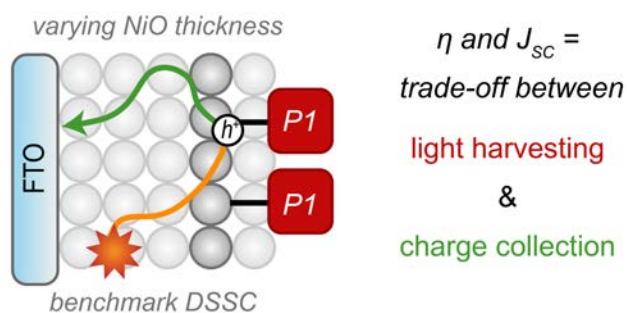
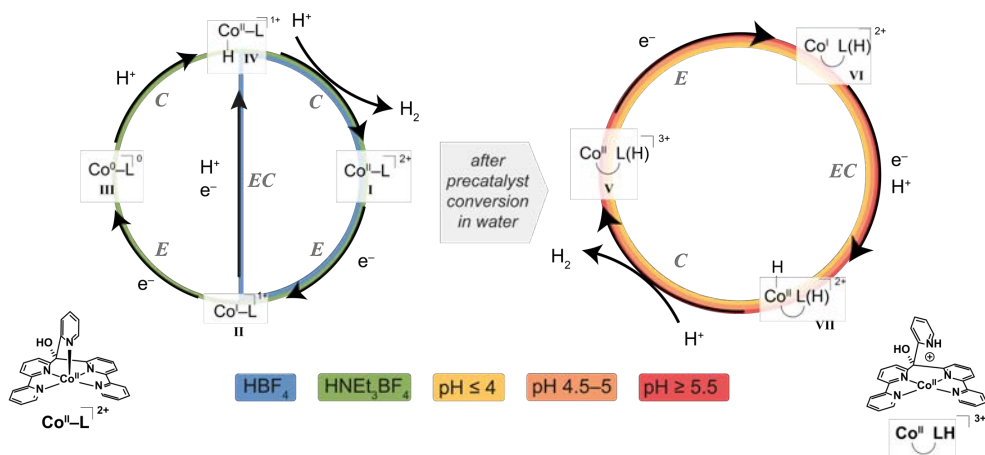


**Figure 2.** A schematic overview of the limiting factors on the solar cell efficiency ( $\eta$ ) and short circuit current ( $J_{sc}$ ) of NiO in the benchmark P1 dye sensitized solar cell. More NiO layers led to an increase in the P1 dye loading, and thus a higher light harvesting efficiency. However, when more NiO layers were applied, the charge collection efficiency decreased (green path), due to the poor hole mobility of NiO, causing relatively more charges to recombine (orange path).

In **Chapter 3**, we studied the mechanism of Co(aPPy), which is one of the most stable molecular catalysts for light-driven proton reduction. Since we plan to carry out light-driven proton reduction in water, we studied the mechanism of the catalyst in both organic and aqueous media, using various electrochemical methods. Cyclic voltammetry in organic and aqueous environments, while varying the acidity of the solution, showed that the catalytic path of the Co(aPPy) proton reduction catalyst can proceed via different routes (Scheme 1). In organic media, in presence of a strong acid ( $\text{HBF}_4$ ), catalysis occurs via an E(EC)C mechanism, whereas in presence of a weaker acid ( $\text{HNET}_3\text{BF}_4$ ), an EECC mechanism is dominating. In aqueous media, the original Co(aPPy) complex was found to be a precatalyst, and we propose that a different species is the active catalyst. One of the pyridine ligands of Co(aPPy) can dissociate in

water and function as a proton relay at  $\text{pH} \leq 5$ . This active species catalyzes proton reduction via an E(EC)C mechanism. These mechanistic findings were in agreement with earlier reported mechanistic studies, and here we could also relate these studies to each other. We then looked into the influence of the mechanism on the stability and deactivation pathways of the Co(aPPy) catalyst. Bulk electrolysis in water showed that the catalyst was most stable in strongly acidic environment, possibly due to the prevention of the formation of the inactive Co–OH species. The catalyst thus functions optimally in strongly acidic aqueous conditions, where the activity and stability are the highest.



**Scheme 1.** Proposed mechanistic pathways under various conditions. Left: catalytic pathways in organic solvents. Right: catalytic pathway in aqueous environment at  $\text{pH}$  3–6, after precatalyst conversion.

In **Chapter 4**, the Co(aPPy) proton reduction catalyst was implemented in a dye-sensitized photocathode, using a novel assembly strategy based on supramolecular interactions (Figure 3). We functionalized the Co(aPPy) catalyst with an alkyl group, which allowed for anchoring to an alkyl-functionalized  $\text{Ru}(\text{bpy})_3^{2+}$  photosensitizer via hydrophobic interactions. After synthesis and assembly of the molecular components on the NiO electrode, the performance of the resulting dye-sensitized photocathode was assessed by various photoelectrochemical techniques. We found an incubation period of approximately 20 minutes before the catalytic activity maximized, which could be rationalized by *in operando* photoelectrochemical impedance spectroscopy, revealing that the catalyst functions as an electron storage site (i.e., capacitor). As a possible explanation for the incubation period, we propose that Co(aPPy) needs to be converted from its precatalytic to its active form.

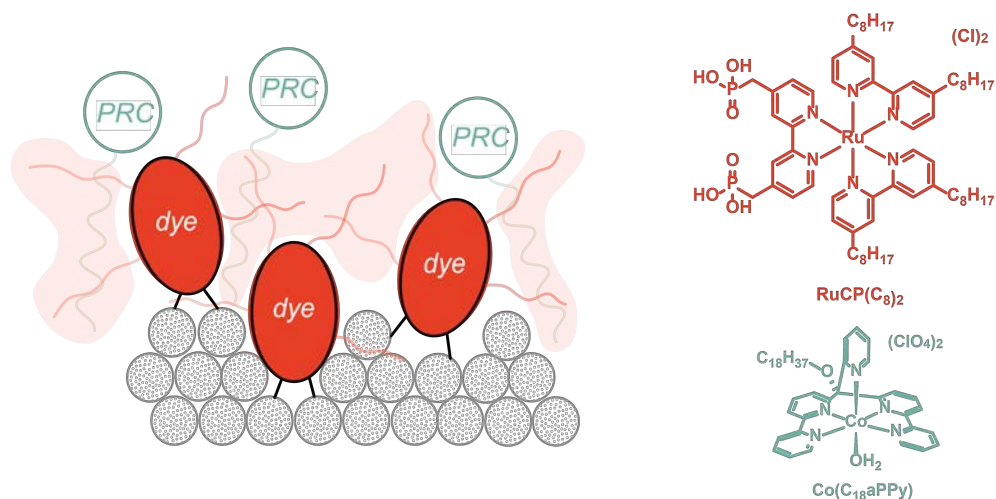


**Figure 3.** Schematic overview of the supramolecular immobilization of the alkyl-functionalized  $\text{Co}(a\text{PPy})$  proton reduction catalyst ( $\text{Co}(\text{C}_{18}\text{aPPy})$ ; PRC) via hydrophobic interactions (orange planes) with the dye ( $\text{RuCP}(\text{C}_8)_2$ ) on the NiO electrode (grey, dotted circles).

In **Chapter 5** we introduce two novel precious metal-free dye-sensitized photocathodes for  $\text{CO}_2$  conversion. The photocathodes are based on the FeTDHPP  $\text{CO}_2$  reduction catalyst, which has been widely recognized as a promising electrocatalyst and photocatalyst, but had not been implemented in a photoelectrode before (Figure 4). Two different approaches were used to assemble the photosensitizer and catalyst on NiO: co-immobilization and supramolecular immobilization. For the co-immobilization, the photosensitizer (C343) and catalyst ( $\text{Fe}-\text{COOH}$ ) were both functionalized with anchoring groups allowing for chemisorption on NiO. The supramolecular immobilization was achieved via hydrophobic interactions between aliphatic groups on the photosensitizer (DPP5) and catalyst ( $\text{Fe}-\text{C}_{12}$ ), similarly to the system described in Chapter 4. Photoelectrochemical studies revealed that the highest photocurrents could be obtained when both the photosensitizers and catalysts were immobilized on the electrode. This proof-of-concept study thus shows that incorporation of the FeTDHPP catalyst in a precious metal-free dye-sensitized photocathode is feasible, both via co-immobilization and supramolecular assembly.

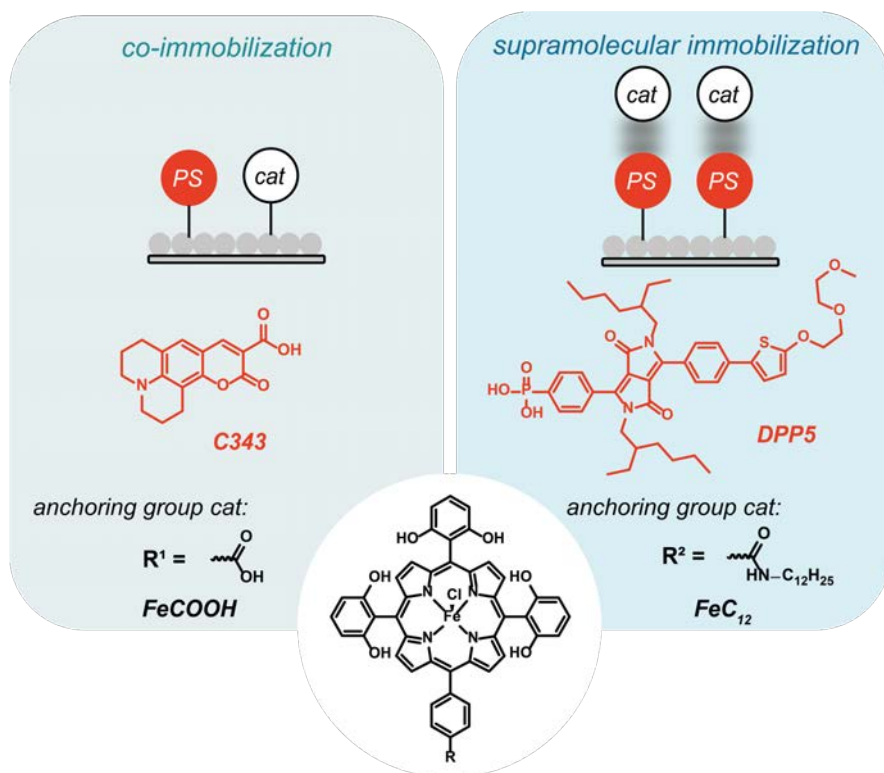


**Figure 4.** Dye-sensitized photocathodes for light-driven  $\text{CO}_2$  reduction. On the left, the co-immobilization approach is shown, using the C343 dye and the Fe-COOH catalyst. On the right, the supramolecular approach is presented, which combines the DPP5 dye with the Fe-C<sub>12</sub> catalyst, which interact via hydrophobic interactions (represented by the dark grey spheres).

Finally, in **Chapter 6**, we further explore the potential of supramolecular immobilization of molecular catalysts on electrodes. Electrochemical  $\text{CO}_2$  reduction by molecular catalysts often encounter mass transfer limitations caused by the poor solubility of  $\text{CO}_2$  and the diffusion of the catalyst. These limitations can be overcome by using gas diffusion electrodes (GDEs), as has been proven for electrochemical  $\text{CO}_2$  reduction with heterogeneous catalysts. Therefore, we immobilized the FeTDHPP catalyst on a carbon nanotube-functionalized GDE via supramolecular  $\pi$ - $\pi$  stacking interactions (Figure 5). The performance of these cathodes were subsequently assessed in an electrochemical flow cell via bulk electrolysis and in-line gas chromatography analysis. We found that the diffusion and mass-transfer limitations could be reduced, since the catalytic activity per FeTDHPP site could be increased 50-fold compared to its activity in solution.

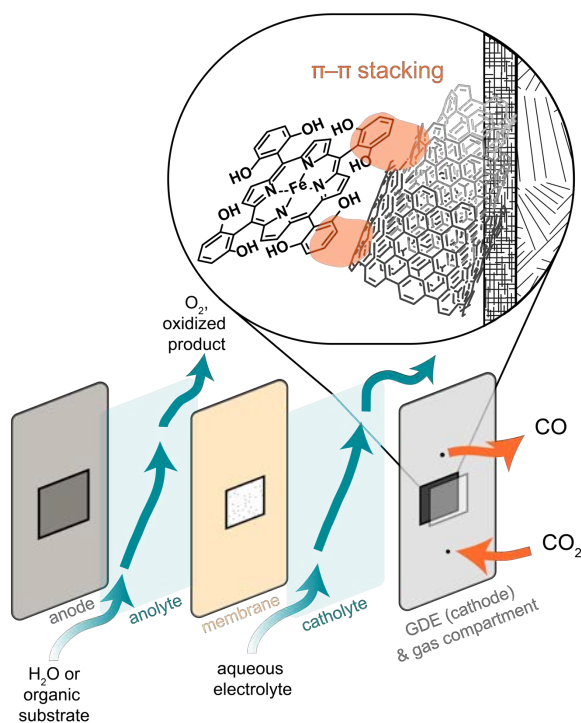


**Figure 5.** Supramolecular immobilization of FeTDHPP onto the GDE in an electrochemical CO<sub>2</sub> reduction flow cell.

Supramolecular immobilization is a versatile strategy to include molecular catalysts on electrodes for solar fuel production. We have shown here that we can install the state-of-the-art molecular first-row transition metal catalysts on (photo)electrodes via self-assembly, using hydrophobic interactions or  $\pi$ - $\pi$  stacking. These novel electrodes were found to be active in (light-driven) proton and CO<sub>2</sub> reduction, underlining the wide applicability of supramolecular immobilization. To further unleash the potential of these novel electrodes for solar fuel production, fundamental challenges regarding the supporting electrode must be addressed, such as background reactivity or poor conductivity, as well as further increasing the stability of the (photo)cathodes. Once the electrodes are able to operate efficiently and reliably, and show a high endurance, artificial photosynthesis and solar fuel production can prosper, and contribute to the energy demands of the future.